Available online at www.derpharmachemica.com

ISSN 0975-413X
CODEN (USA): PCHHAX

Der Pharma Chemica, 2017, 9(19): 1-8
(http://www.derpharmachemica.com/archive.html)

Synthesis, Characterization, XRD Studies, Molecular Docking and Biological Screening of N-phenyl-2-(pyridin-4-ylcarbonyl) Hydrazine Carboxamide and their 3d Metal Ion Complexes

Yuvaraj TCM[1*], Parameshwara Naik P[1], Krishnamurthy G[1], Venkatesh TV[2], Mohammed Shafeeulla R[1], Manjuraj T[1]

[1]*Department of Chemistry, Sahyadri Science College (Auto), Shimoga, Karnataka, India*
[2]*Department of Chemistry, Kuvempu University, Shankaraghatta, Karnataka, India*

ABSTRACT

A synthesis of semicarbazide derivative like N-phenyl-2-(pyridin-4-ylcarbonyl) hydrazine carboxamide by the reaction of isoniazid and phenyl isocyanate has been done, using this ligand and their 3d metal ions such as Ni^{II}, Co^{II}, Cu^{II}, Zn^{II} and Mn^{II} complexes were synthesized. The ligand and their metal complexes have been characterized by different analytical techniques, such as elemental analyses, molar conductivity measurements, UV-Visible, Fourier Transform Infra-Red (FTIR), Proton Nuclear Magnetic Resonance (^{1}H-NMR), Carbon-13 Nuclear Magnetic Resonance (^{13}C-NMR), Liquid Chromatography–Mass Spectrometry (LCMS), Powder X-ray Diffraction (PXRD) and Thermo Gravemetric Analysis (TGA) studies. The antioxidant, antimicrobial and antifungal activity of these compounds reported agreeable results against bacterial strains and fungal strains. The molecular docking studies for synthesized complexes exhibited excellent binding energy interaction with protein enzymes.

Keywords: Semicarbazone derivative, Thermal analysis, Microbial activity, XRD, Molecular docking

INTRODUCTION

The most common traditional method for the synthesis of the semicarbazone derivatives is obtained by reaction of R-CO-NH-NH_2 and R-NCO. Most complexes of semicarbazone derivatives behave as bidentate ligands because they can bind to metals through oxygen and the hydrazine nitrogen atoms, although in some cases they behave as unidentate ligands by binding through an only nitrogen atom [1,2]. Semicarbazone plays a main key role in organic and biological chemistry. The semicarbazone linkage is an important functional group due to its extensive presence in natural products, pharmaceutical compounds and synthetic polymers. Transition metal ions are playing an important role in biological processes in the human body. For example, nickel(II), copper(II) and zinc(II) ions are the most abundant transition metals in humans [3-5]. Recent years, more number of studies devoted to search derivatives of semicarbazides and studied their chemical and structural properties and potential biological activities such as antimicrobial, antioxidant, anticancer, antitubercular, antimalarial, antitumor, sodium channel blocker, antiviral and antifungal activities [6-8]. Moreover, semicarbazone derivatives have found their way into almost every branch of chemistry; commercially they are used as dyes, photographic films, plastic and in the textile industry [9,10]. The semicarbazone linkage is an important functional group due to its extensive presence in natural products, pharmaceutical compounds, and synthetic polymers [11]. The above properties of semicarbazone derivative and their complexes led us to synthesize some new compounds of such type and investigate their properties in greater detail. Also, all the synthesized complexes were investigated for molecular docking and the *in vitro* antioxidant activity.

MATERIALS AND METHODS

The chemicals isoniazid, phenyl isocyanate, CH_3COOH and acetone were purchased from the Sigma-Aldrich, Laboratory chemicals, Bangalore, Karnataka, India. Nickel(II) chloride hexahydrate, cobalt(II) chloride hexahydrate, copper(II) chloride dehydrate, anhydrous zinc(II) chloride and manganese(II) chloride were purchased from Merck. The metal chlorides were used in their hydrated form. The ethanol, methanol and acetone were distilled and dried by following the reported method [12].

Synthesis of N-phenyl-2-(pyridin-4-ylcarbonyl) hydrazine carboxamide (IP)

The calculated amount of isoniazid (2.05 g, 0.015 mol) and phenyl isocyanate (1.43 g, 0.012 mol) were dissolved in 20 ml dry acetone with one drop of acetic acid. The resulting mixture was stirred on a magnetic stirrer at about 500 rpm for 12 h at 60°C. The progress of a reaction was monitored by TLC (n-Hexane:Ethyl acetate in the ratio 0.7:0.3). After the reaction, the reaction product was poured into ice cold water when the

ivory white colored precipitate obtained which was filtered, washed with excess water for five times, dried and recrystallized from the ethanol (Schemes 1 and 2).

$C_{13}H_{12}N_4O_2$: Yield: 72%; Colour: Ivory white; m.p: 180-182°C; M.W: 256.25; Anal. Calcd. and found for (%): C-60.93 (60.99), H-4.72 (4.82), N-21.86 (21.89), O-12.49, IR (KBr, cm^{-1}): 3250 (N_4-H), 3109 (N_3-H), 2976 (N_1-H), 2891 (Ar-C-H), 1670 (C_2=O), 1596 (C_5=O), 1071 (N-N). ^{1}H-NMR (DMSO-d_6, 400 MHz), δppm=10.84 (s, 1H, N_4H), 9.86 (s, 1H, N_3H), 9.79 (s, 1H, N_1H), 7.15-7.35 (t, 3H, 1-benzene), 7.42-7.44 (d, 2H, 1-benzene), 7.84-7.85 (d, 2H, 4-phyridine), 8.76-8.78 (d, 2H, 4-phyridine). ^{13}C-NMR (100 MHz, DMSO-d_6), δppm=180.55 (C_5=O), 164.55 (C_2=O), 121.68, 125.20, 125.86, 127.96, 128.09 (6C, 1- benzene). 129.90, 139.07, 139.62, 150.14 (5C, 4-pyridine). Mass spectrum (M^+) at m/z: 256.25 (256.90) (Figures 1 and 2).

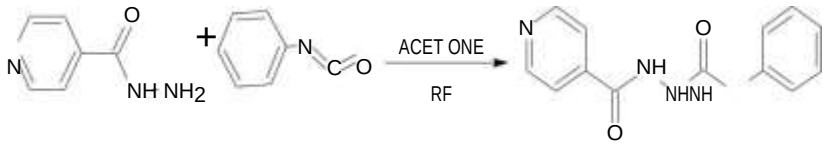

Scheme 1: Synthesis of IP ligand

Synthesis of the metal complexes

A solution of nickel(II)chloride hexahydrate (0.713 g, 0.003 mol), cobalt(II) chloride hexahydrate (0.713 g, 0.003 mol), copper(II) chloride dehydrate (0.511 g, 0.003 mol), zinc(II) chloride (0.408 g, 0.003 mol) and manganese(II) chloride tetrahydrate (0.593 g, 0.003 mol) in 20 ml ethanol was added to a solution of IP (1.741 g, 0.003 mol) in 10 ml ethanol. The resulting reaction mixture was refluxed for 8 h to obtain corresponding metal complexes. The solid product was collected by filtration and washed with 4-5 ml of hot methanol and dried in a vacuum over anhydrous calcium chloride in desiccators. The obtained metal complexes were characterized by melting point, molar conductance, and spectral techniques.

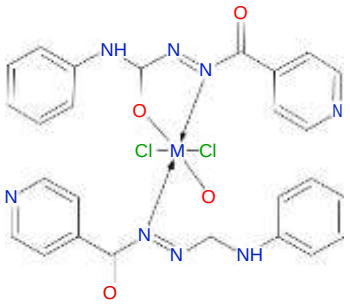

Scheme 2: Proposed structure of metal complex (M=Ni^{II}, Co^{II}, Cu^{II}, Zn^{II} and Mn^{II})

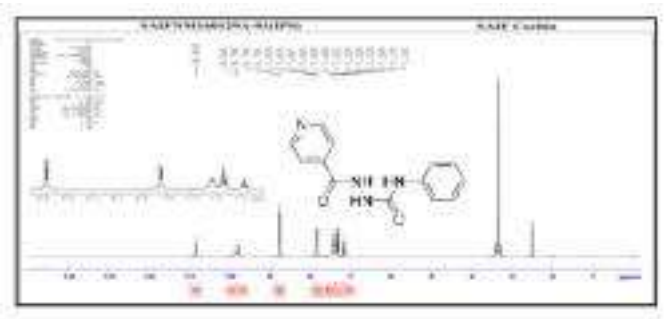

Figure 1: ^{1}H-NMR spectrum of IPS

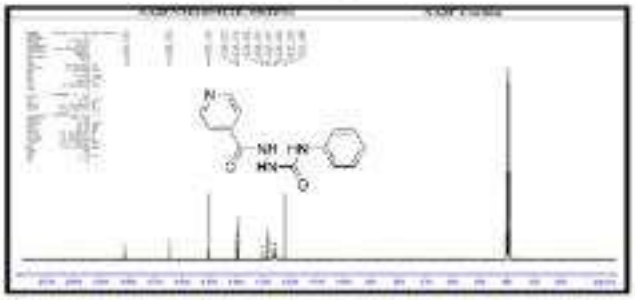

Figure 2: ^{13}C-NMR spectrum of IPS

$[Ni(L)_2]Cl_2.2H_2O$ complex (IP_1): $C_{26}H_{22}Cl_2N_8NiO_4.2H_2O$; Yield: 64%; Colour: Dark green; m.p: 298-300°C; M.W: 676.10; Anal. calcd and found for (%): C-48.79 (48.89), H-3.46 (3.66), N-17.42 (17.51), O-10.00, Ni-9.17. IR (KBr, cm^{-1}): 3193 (ν_{H2O}), 2977 (N^1-H), 2890 (Ar-H), 1560 (C_5=O), 1524 (N=N), 454 (M-O), 430 (M-N). Molar conductance: 104.70 $ohm^{-1}.cm^2.mol^{-1}$.

Physical measurements

The elemental analyses (C, H, N, S) was performed using Perkin-Elmer 2400 II C, H, N, S and O elemental analyzer and the metal analyses were carried out by standard methods. The melting point of the ligand and their metal complexes was measured by using melting point apparatus model code NAMPA/045. UV-Visible spectra were measured in Dimethylformamide (DMF) or Dimethyl Methyl Sulfoxide (DMSO) on an ocean optics USB 4000USA spectrophotometer, using 1 cm path length cuvette at room temperature. Infrared spectra were recorded using Fourier Transform Infra-Red (FTIR) 8400s Shimadzu spectrometer with KBr pellets in the range of 400-4000 cm^{-1}. The molar conductance data was measured using freshly prepared DMF solutions (10^{-3}M) at 25°C with an EQUIP-TRONICS model-660A instrument. The NMR spectra have been recorded as 400 MHz Varian-AS NMR spectrometer in DMSO-d_6 using Tetramethylsilane (TMS) as the internal standard. The Differential Thermal Analysis (DTA) and Thermogravimetric Analysis (TGA) of compounds were carried out on a Shimadzu DT-30 and TG-50 thermal analyzers in the range 27-900°C at the heating rate of 10°C/min in nitrogen atmosphere 80.0 ml/min. The magnetic susceptibility values measured at the room temperature using the Gouy method with mercuric Tetrathiocyanatecobaltate(II) as the standard. Mass spectra were recorded using the instrument Code; SC/AD/10-014.

RESULTS AND DISCUSSION

The reaction of metal chlorides and semicarbazone derivative in ethanol in 1:2 molar ratio results in the formation of corresponding complexes. The resulting complexes are insoluble in common organic solvents, but soluble in DMF and DMSO. The elemental analyses results were in good agreement with the proposed formula of the complexes. The molar conductance value of IP_4 was slightly higher due to partial dissociation of complexes in their solution, indicating the non-electrolytic nature, In the case of other complexes showed uni-bivalent nature.

Nuclear magnetic resonance (NMR) studies

In the case of ^{1}H-NMR spectrum of the IP, the signals at 9.79, 9.86 and 10.84 ppm (s, 3H, NH) is assigned to NH protons of semicarbazide group. The aromatic hydrogen resonance observed at 7.15-7.35 (t, 3H, Ar-H) and 7.42-7.44 ppm (d, 2H, Ar-H). In addition, the doublets around 7.84-8.78 ppm (d, 4H, Ar-H) are due to 4-pyridine ring protons. ^{13}C-NMR spectrum of IP exhibited signals at 164.55 and 180.55 ppm assigned to two (C=O) groups, respectively. 1-benzene and 4-pyridine moieties exhibited peaks in the region 121.68-128.09 and 129.90-150.14 ppm, respectively. The mass spectrum confirms the formula of IP by giving molecular ion peak (M^+) corresponding to their molecular weight. The mass spectrum of uncoordinated IP was presented in Figure 3.

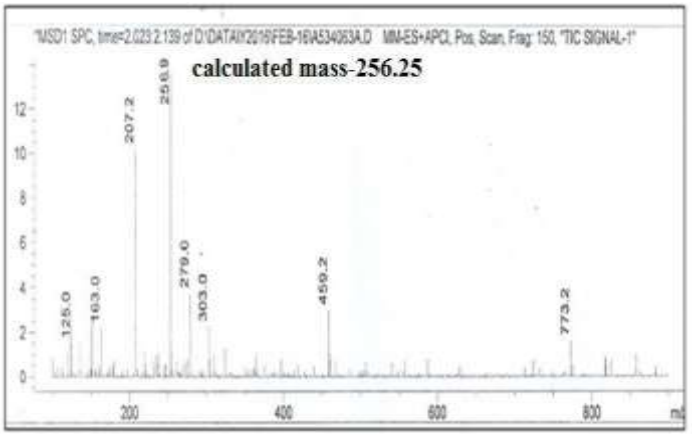

Figure 3: Liquid chromatography-mass spectrum of IPS

Fourier transform infra-red (FTIR) spectral studies

The IR spectrum of IP indicated strong intensity bands at 2976 (N_1-H), 3109 (N_3-H) and 3250 (N_4-H) cm^{-1} assignable to ν_{NH} of semicarbazide group [13,14]. In the case of IR spectrum of metal complexes, the band due to two NH groups of semicarbazide have been disappeared, indicating enolization of the C=O during complexation and the subsequent coordination of the carbonyl oxygen by deprotonation [15**].** The absence of two NH groups and a single band at 2977 (N^1-H) cm^{-1} due to NH group in the metal complexes and appearance of a new band at 1547 cm^{-1} indicate -N=N-bond formation. The new band appeared in this involvement suggest oxygen of semicarbazide in the complexation with metal ions [16]. The appearance of new bands around 3185, 3193 and 3249 cm^{-1} in the spectrum of complexes indicate the presence of lattice water [17]. The bands appeared in the spectrum of complexes IP_1-IP_5 in the region 448-467 and 416-430 cm^{-1} are due to ν_{M-O} and ν_{M-N} respectively [18,19].

Electronic absorption spectra and magnetic moment

In the electronic spectrum of wine red coloured Co^{II} complex, three ligand field bands observed at 14,925, 16,393 and 18,181 cm^{-1} due to the $^4T_{1g}(F) \rightarrow {}^4T_{2g}(F)$ (ν_1), $^4T_{1g}(F) \rightarrow {}^4A_{2g}(F)$ (ν_2) and $^4T_{1g}(F) \rightarrow {}^4T_{1g}(P)$ (ν_3) transitions, respectively [20,21]. The observed magnetic moment value was 3.92 BM and also supports the complex to have octahedral geometry. The spectrum of dark green colored Ni^{II} complex showed bands at 23,809 cm^{-1}, corresponding to $^1A_{1g} \rightarrow {}^1B_{1g}$, ($\nu_1$) and $^1A_{1g} \rightarrow {}^1B_{2g}$ (ν_2) transitions [22]. The IP_1 complex exhibits one band and diamagnetic was due to square planar geometry. The Cu^{II} showed the band at 15,625 cm^{-1}, which may be assigned to the transitions $^2B_{1g} \rightarrow {}^2A_{1g}$ ($d^2x-y_2 \leftarrow d^2z$) (ν_1) [23]. The light broad band of green colored IP_3 showed the magnetic moment value 1.90 BM indicative of distorted octahedral geometry. The Mn^{II} complex exhibits a band of weak intensity at 10,309 cm^{-1} and its magnetic moment value 5.82 BM, which may be assigned

to $^6A_{1g} \rightarrow {}^4T_{1g}$ transition in a distorted octahedral environment [24]. The comparison study of UV- spectra of IP and IP_1-IP_3 are presented in Figure 4.

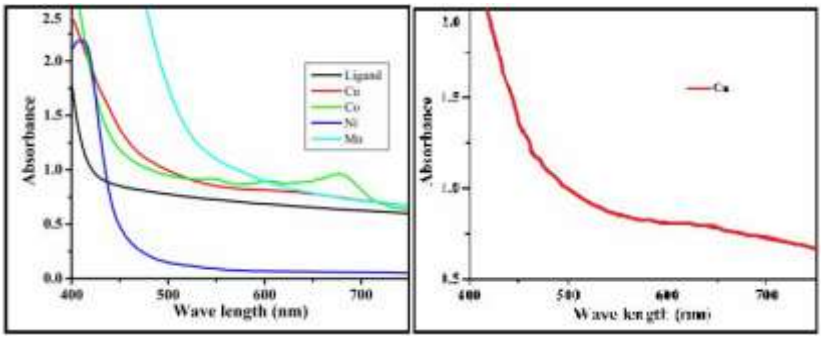

Figure 4: Electronic spectra of IP and IP_1-IP_5

Thermal analyses studies of metal complexes

Thermal stability and thermal behaviors of all complexes were studied by TGA in the temperature range 25-900°C. The thermogram of the IP_1 shows a mass loss of calcd: 5.32% (Found: 5.52%) in the temperature range 95-110°C indicates the loss of two lattice water molecules. The second step of the decomposition from 160-250°C, with a mass loss of 10.50% (10.25%) corresponds to loss of the coordinated two chlorine atoms, the third step involves in the dissociation at the temperature of 260-380°C with weight loss of 34.93% (34.44%) corresponds to the decomposition of pyridine moiety [25,26]. The fourth step at 400-620°C with weight loss of found 38.20% (37.23%) is referring to the removal of phenyl isocyanate moiety and at the end, left was stable residue NiO 11.04% (10.54%) at 600-750°C. Similarly, the thermogram of the IP_3 and IP $_5$ show a mass loss of 2.71, 2.75% (3.01, 2.99%) in the temperature range 95-120°C indicates the loss of one lattice water molecules. Also, the TG curves of the IP_2-IP_5 showed three steps of decomposition. The first step at 180-240, 150-240, 180-260 and 170-280°C with weight loss of 11.08, 10.70, 10.97 and 10.85% (10.56, 10.99, 11.18 and 11.12%) is attributed to the loss of the two chlorine atoms, the second step with weight loss of 36.88, 35.62, 36.51 and 36.09% (36.12, 34.92, 35.99 and 35.89%) at 270-350, 250-370, 280-380 and 260-390°C was corresponding to the removal of pyridine moiety. The third step at 320-680, 340-690, 400-700 and 390-700°C with a weight loss of 40.42, 38.96, 39.93 and 39.42% (39.36, 37.56, 38.56 and 38.92%) is referring to the removal of phenyl isocyanate moiety. The mass of the final residue 11.61, 11.99, 12.58 and 10.83% (10.92, 12.03, 13.14 and 11.14%) at 700-750, 700-760, 720-740 and 690-750°C corresponded to stable CoO, CuO, ZnO and MnO [27]. The results well agreed with the proposed structure of metal complexes. The nature of decomposition curves of IP_1-IP_5 is represented in Figure 5.

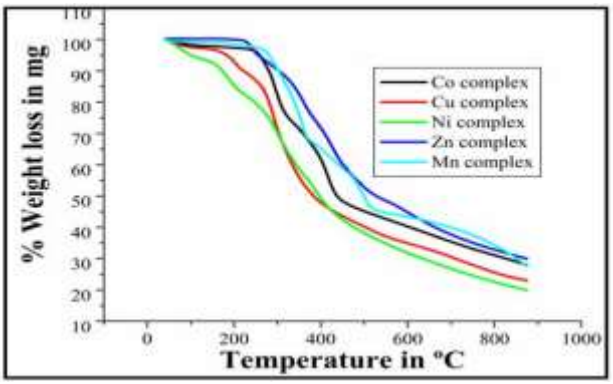

Figure 5: Thermo gravimetric analysis thermogram of IF_1 to IF_5

Antioxidant and antimicrobial evaluation of IP and their metal complexes

DPPH Free radical scavenging activity

Antioxidant activity of different concentration of complexes in DMF and ascorbic acid in terms of free radical scavenging ability was evaluated using DPPH free radical assay **[**28**].** The compounds exhibited marked antioxidant activity by scavenging DPPH• (free radical) and converting into DPPH and the activity was found to be dose dependent (Figure 6). Among the synthesized complexes IP_1, IP_3 and IP_5 exhibited excellent inhibition activity, while the other complexes showed moderate antioxidant activity. The complexes IP_1-IP_5 found to be more potent than the IP. The results are given in Table 1.

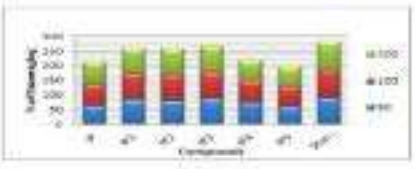

Figure 6: Antioxidant activity of IP and their metal complexes

Table 1: DPPH free radical scavenging activity of IP and their metal complexes

Compounds	DPPH radical scavenging activity (%) of different concentrations (g/ml) of compounds		
	50	**100**	**200**
IP	64.28	71.05	76.78
IP_1	83.94	87.19	87.42
IP_2	82.76	87.14	91.12
IP_3	88.56	88.56	83.54
IP_4	76.29	70.25	73.74
IP_5	65.17	66.99	69.54
Standard	93.33	93.80	93.10

Antibacterial activity of IP and their metal complexes

A cup plate method using Hi-Media agar medium was employed to study the antibacterial activity of the synthesized compounds against three Gram-positive bacteria, *Staphylococcus aureus*, *Streptococcus pyogenes* and *Propionibacterium acnes* and three Gram-negative bacteria, *Escherichia coli*, *Klebsiella terrigena* and *Klebsiella pneumoniae*. Preparation of nutrient broth, subculture, base layer medium, agar medium and peptone water was done as per the standard procedure [29]. The compounds IP_1, IP_3 and IP_5 showed promising antibacterial activity against tested organism compared with standard tetracycline. The results of the study are summarized in Table 2.

Table 2: Antibacterial activity of IP and its complexes

Entry	Concentration µg/ml	Zone of inhibition(mm)					
		Gram-positive bacteria			Gram-negative bacteria		
		Staphylococcus aureus	***Streptococcus pyogenes***	***Propionibacterium acnes***	***Escherichia coli***	***Klebsiella terrigena***	***Klebsiella pneumoniae***
IP	50	13	12	10	11	12	10
	100	13	13	11	12	14	11
	200	15	15	14	13	14	15
IP_1	50	13	13	11	15	12	15
	100	14	14	12	14	15	14
	200	14	13	16	16	17	12
IP_2	50	12	11	15	11	10	14
	100	14	15	12	16	13	14
	200	14	15	16	17	15	15
IP_3	50	12	14	13	11	11	10
	100	16	15	14	16	12	13
	200	17	15	16	15	15	15
IP_4	50	13	12	10	11	11	13
	100	14	12	13	13	14	15
	200	14	13	14	14	15	14
IP_5	50	12	11	13	12	11	10
	100	13	13	14	15	13	13
	200	14	15	16	17	15	16
Control	-	00	00	00	00	00	00
Tetracycline	-	22	19	22	21	20	22

Antifungal activity of IP and their metal complexes

The antifungal activity of the synthesized compounds was tested against three different fungi, i.e., *Candida albicans, Candida neoformans and Trichosporon* by a filter paper disc technique [30]. The concentration of test compounds was 50-200 µg/ml. After 48 h treatment, the zone of inhibition produced by each compound was measured in mm. Fluconazole was used as the standard antifungal agent and DMF as a control. Moreover, the microbial data revealed that the complexes are superior to the free ligand in the inhibition of the tested bacteria and fungi. It is noticed that the concentration play a vital role in increasing the degree of inhibition, i.e., the activity increased with increasing concentration of the complexes. The antifungal activity was also carried out against three fungal strains. The potent activity exhibited by the compounds IP_1, IP_3 and IP_5 compared with the standard drug fluconazole (Figures 6-9). The results are described in Table 3.

Molecular docking studies

Molecular modeling studies were performed by using *Hex* 8.2 protein-ligand docking in Protein Data Base (PDB) formats. The parameters used for docking include correlation type-shape only, FFT mode 3D, grid dimension 0.6, receptor range 180, ligand range 180, twist range 360, distance range 40. The starting coordinates of the human antioxidant enzyme in complexes with the competitive inhibitor DTT (PDB: 3MNG) were taken from the PDB (http://www.rcsb.org/pdb) [31]. The ligand was docked against the lead competitive inhibitor ligand Dithiothreitol (DTT) at the crystal enzyme structure of the target protein and the best energy conformations of receptor ligand were studied and the energy of binding was calculated as the difference between the energy of the complex and the individual energies of enzyme and the ligand
[32]. In order to interrupt the binding interactions modes, *in vitro* of IP and metal complexes with a human antioxidant enzyme in complexes with the competitive inhibitor DTT (PDB: 3MNG). The binding energy of all the complexes showed prominent binding interactions, Ni^{II} complex gives the highest binding energy of -308.11 kcal/mol, while Co^{II}, Cu^{II}, Zn^{II} and Mn^{II} complexes showed -291.89, -291.85, -281.59 and -293.81 kcal/mol with human antioxidant 3MNG protein receptor by the key of amino acid residues PHE128, LEU97, VAL39, LEU110, LEU125, GLY38, ARG127, HIS51, PHE37, GLY38, ARG127, HIS51, LEU36, VAL39, LEU125, LEU96, CYS72, LEU97, GLY38, ARG127, PHE37, MET130, LEU36, PHE29, ALA71, LEU97, VAL39, PRO40, LEU125, ARG127 and LEU36. The hydrophobic and hydrophilic spheres are used to recognize the interactive positions which will be the potential ligand binding sites in each possible position. Finally, the molecular docking studies for the selected compounds revealed that the synthesized compounds are antioxidant competitive inhibitors in comparison to antioxidant inhibitor DTT at a 3MNG binding receptor (Table 4).

Table 3: Antifungal activity of IP and IP_1-IP_5

Entry	Concentration µg/ml	Zone of inhibition (mm)		
		Candida albicans	*Candida neoformans*	*Trichosporon*
IP	50	11	10	11
	100	11	12	11
	200	13	13	12
IP_1	50	12	11	12
	100	14	13	14
	200	16	15	16
IP_2	50	12	11	12
	100	14	14	12
	200	17	15	16
IP_3	50	13	11	10
	100	14	13	13
	200	15	14	15
IP_4	50	12	12	10
	100	13	14	13
	200	16	17	15
IP_5	50	11	12	13
	100	14	14	15
	200	17	15	16
Control	-	0	0	0
Fluconazole	10	23	22	21

Table 4: Molecular docking studies of IP and IP_1-IP_5

Compounds	Receptor PDB code	ΔG (kcal/mol)
IP	3MNG	-170.89
IP_1	3MNG	-308.11
IP_2	3MNG	-291.89
IP_3	3MNG	-291.85
IP_4	3MNG	-287.59
IP_5	3MNG	-293.81

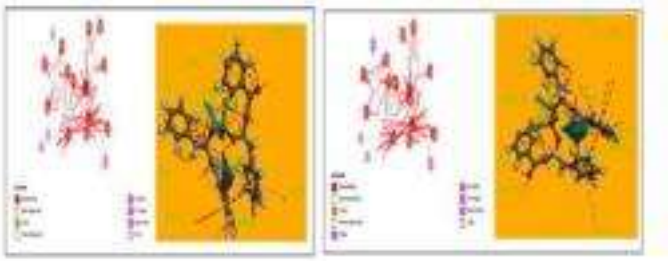

Figure 7: Three dimensional (3D) and two dimensional (2D) interactions of compounds IP_1 with active site of receptor 3MNG

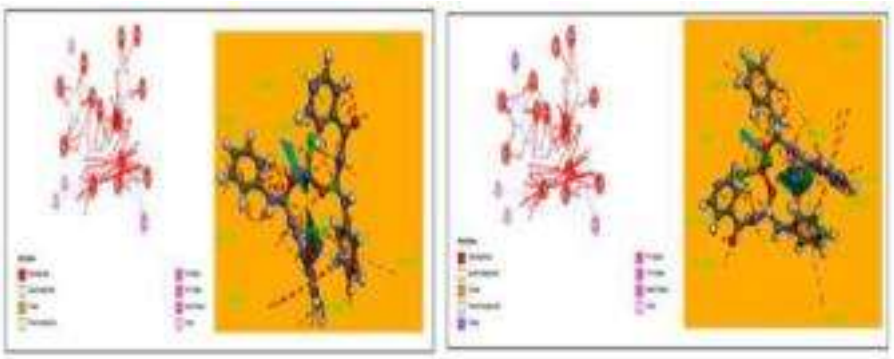

Figure 8: Three dimensional (3D) and two dimensional (2D) interaction of compounds (b) IP_2 and (c) IP_3 with active site of receptor 3MNG

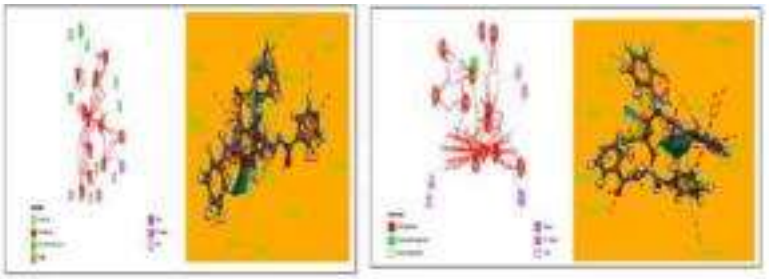

Figure 9: Three dimensional (3D) and two dimensional (2D) interaction of compounds (d) IP_4 and (e) IP_5 with active site of receptor 3MNG

Powder X-ray diffraction (PXRD) studies

The powder X-RD diffraction is carried out for complexes IP_4 and IP_5 which show prominent sharp peaks while the complexes IP_1-IP_3 showed no peaks, indicating amorphous nature [33]. The diffraction patterns of the complexes given in Figure 10. The Miller indices (hkl) along with observed and calculated d angles, 2θ values are given in Tables 5 and 6. The average crystalline sizes of the IP_4 and IP_5 complexes dxrd were calculated using Debye-Scherer equation (D=Kλ/β Cos θ, where, D=Particle size, K=Dimensionless shape factor, λ=X-ray wavelength (0.15406Å) β=Line broadening at half the maximum intensity, θ=Diffraction angle [34,35]. The complexes IP_4 and IP_5 have a crystalline size of 32.34 and 37.23 nm respectively, suggesting that the complexes are in a nanocrystallite phase.

Table 5: PXRD spectral data of IP_4 complex

Peak No.	2θ	θ	Sinθ	hkl	d in Å		a in Å
					Observation	Calculation	
1	12.3462	6.1731	0.1075	850	7.16335	7.1627	3.6965
2	14.0975	7.0487	0.1227	862	6.2772	6.2754	3.6965
4	15.3715	7.68575	0.1337	450	5.7596	5.7591	3.6965
5	16.1571	8.07855	0.1405	998	5.4813	5.4803	3.6965
6	18.1834	9.0917	0.1580	466	4.8748	4.8076	3.6965
7	21.8042	10.9021	0.1891	240	4.0728	4.0710	3.6965
8	23.3546	11.6773	0.2083	547	3.8058	3.8065	3.6965
9	24.0565	12.02825	0.2186	995	3.6963	3.6965	3.6965
10	25.7754	12.8877	0.2430	949	3.4536	3.4529	3.6965
11	28.1371	14.06855	0.2847	600	3.1688	3.1687	3.6965
12	33.0893	16.54465	0.3083	208	2.7050	2.7046	3.6965
13	35.9238	17.9619	0.3167	396	2.4978	2.4975	3.6965
14	38.2329	19.11645	0.3354	455	2.3521	2.3527	3.6965
15	39.2027	19.60135	0.3621	522	2.2961	2.2951	3.6965
16	42.4674	21.2337	0.3819	508	2.1268	2.1264	3.6965

Table 6: P-XRD spectral data of IP_5 complex

Peak No.	2θ	θ	Sinθ	hkl	D in Å		a in Å
					Observation	Calculation	
1	16.8376	8.4188	0.1464	731	5.26132	5.2595	4.6912
2	18.4851	9.2425	0.1606	389	4.79593	4.7945	4.6912
4	19.0456	9.5228	0.1654	218	4.65605	4.6550	4.6912
5	20.4978	10.2489	0.1779	431	4.32934	4.3282	4.6912
6	20.9729	10.4864	0.1820	241	4.23233	4.2307	4.6912
7	21.3462	10.6731	0.1852	262	4.15915	4.1576	4.6912
8	27.1412	13.5706	0.2346	666	3.28284	3.2821	4.6912
9	27.8299	13.9149	0.2406	824	3.20314	3.2001	4.6912
10	28.5603	14.2801	0.2466	710	3.12287	3.1220	4.6912
11	29.0023	14.5011	0.2503	340	3.07627	3.0760	4.6912
12	29.4491	14.7245	0.2541	276	3.03061	3.0303	4.6912
13	30.3364	15.1682	0.2616	248	2.94395	2.9434	4.6912
14	31.7078	15.8539	0.2731	337	2.81968	2.8194	4.6912
15	33.3039	16.6519	0.2865	446	2.68811	2.6876	4.6912
16	39.0519	19.5259	0.3342	422	2.30467	2.3040	4.6912

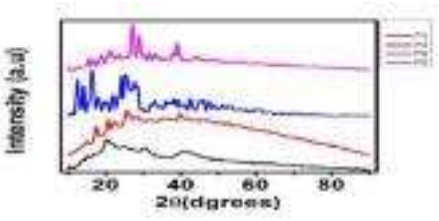

Figure 10: Powder X-ray diffraction spectra of IP_1-IP_4

CONCLUSION

In the present work, the ligand and a series of its metal complexes from IP_1-IP_5 have been synthesized. These compounds are characterized by various physicochemical techniques. The TGA/DTA data indicate stepwise degradation. The obtained results are in good agreement with the proposed structure. Ligand behaves as a bidentate ligand and coordinates through nitrogen and carbonyl oxygen atoms. The two chlorine atoms also occupy the two sites of each metal giving a distorted octahedral geometry for Mn^{II}, Zn^{II} and Cu^{II} complexes. However, N(II) and CO(II) complexes are distorted square planar and octahedral geometry, respectively. The newly synthesized IP_1-IP_5 exhibited moderate antibacterial activity against *S. aureus*, *S. pyogenes*, *P. acnes*, *E. coli*, *K. terrigena* and *K. pneumoniae* and significant antifungal activity against *C. albicans*, *C. neoformans* and *Trichosporon.* The complexes exhibited excellent binding energy interactions with protein enzymes towards molecular docking.

ACKNOWLEDGEMENT

The authors thank the University Grant commission, New Delhi for financial support for providing research facilities as well as the Principal, Sahyadri Science College (Auto), Shivamogga. The authors also thank the Kuvempu University for providing facility and the SAIF for spectral analysis, Cochin.

REFERENCES

[1] S.N. Pandeya, P. Yogeeswari, J.P. Stables, *Eur. J. Med. Chem*., **2000**, 35, 886.
[2] S.N. Pandeya, V. Mishra, P.N. Singh, D.C. Rupainwar, *Pharm. Res*., **1998**, 37, 22.
[3] Kaim, Schwederski B, *Bioinorg. Chem*., **1996**, 39-262.
[4] C. Xiao-Ming, Y. Bao Hui, C.H. Xiao, X.J. Zhi Tao, *Chem. Soc*., **1996**, 3465-3468.
[5] F.A. Cotton, G. Wilkinson, *Adv. Inorg. Chem*., **1988**, 1358-1371.
[6] T. Hemalatha, P.K.M. Imran, A. Gnanamani, S. Nagarajan, *Biol. Chem*., **2008**, 19, 311.
[7] K. Alomar, V. Gaumet, M. Allain, G. Bouet, A. Landreau, *J. Inorg. Biochem*., **2012**, 115, 43.
[8] P.F. Lee, C.T. Yang, D. Fan, J.J. Vittal, J.D. Ranford, *Polyhedron*., **2003**, 22, 2781.
[9] J. Patole, S. Dutta, S. Padhey, E. Sinn, *Inorg. Chim. Acta*., **2001**, 318, 207.
[10] R. Sharma, S.K. Agarwal, S. Rawat, M. Nagar, *Trans. Met. Chem*., **2006**, 31, 201.
[11] Z. Afrasiabi, E. Sinn, W. Lin, Y. Ma, C. Campana, S. Padhye, *J. Inorg. Biochem*., **2005**, 9, 1526.
[12] S.A. Galal, K.H. Hegab, A.S. Kassab, M.L. Rodriguez, S.M. Kerwin, A.M.A.E Khamry, H.I.E Diwani, *Eur. J. Med. Chem*., **2009**, 44, 1500.
[13] V. Haribabu, P.V. Anantha Lakshmi, V. Jayatyaga Raju, *Int. J. Chem. Tech. Res*., **2013**, 5, 1518.
[14] R.S. Baligar, V.K. Revankar, *J. Serb. Chem. Soc*., **2006**, 71, 1310.
[15] P.V. Anantha Lakshmi, P. Saritha Reddy, V. Jayatyaga Raju, *Spectrochem. Acta*., **2009**, 74, 52-57.
[16] P.V. Anantha Lakshmi, B.S. Shyamala, V. Jayatyaga Raju, *J. Chem*., **2009**, 83, 1563.
[17] D. Sandhya Rani, P.V. Anantha Lakshmi, V. Jayatyaga Raju, *Res. J. Pharm. Biol. Chem. Sci*., **2014**, 5, 1304-1314.
[18] A. Koji, M. Kanako, O. Masaki, O. Hishashi, *Inorg. Chem*., **2002**, 41, 4461.
[19] R. Malhotra, S. Kumar, Jyoti, H. R. Singal, K. S. Dhindsa, *Ind. J. Chem*., **2000**, 39, 421.
[20] A.M.A. Alaghaz, H.A. Bayoumi, Y.A. Ammar, S.A. Aldhlmani, *J. Mol. Struct*., **2013**, 1035, 399.
[21] F.A. Cotton, G. Wilkinson, *Adv. Inorg. Chem*., **1972**.
[22] I.C. Lavos-Valereto, S. Wolynec, I. Ramires, A.C. Guastaldi, I. Costa, *J. Mater. Sci. Mater. Med*., **2004**, 15, 59.
[23] S.R. Gupta, P. Mourya, M.M. Singh, V.P. Singh, *J. Organomet. Chem*., **2014**, 767, 143.
[24] M. Mishra, K. Tiwari, A.K. Singh, V.P. Singh, *Inorg. Chim. Acta*., **2015**, 425, 36-45.
[25] S. Khan, S.A.A. Nami, K.S. Siddiqi, *J. Mol. Struct*., **2008**, 875, 478-485.
[26] D, Ascenzo, G. Wendlendt, *J. Therm. Anal*., **1969**, 1, 423-434.
[27] A.M. Donia, M.M. Gouda, M.I. Ayad, H.A. ElBoraey, *Thermochim. Acta*., **1992**, 194, 155.
[28] S.B Patil, G. Krishnamurthy, M.R. Lokesh, N.D. Shashikumar, H.S.B Naik, R.L Prashant, M. Ghate, *Med. Chem. Res*., **2012**, 21, 3327.
[29] N.D. Jayanna, H.M. Vagdevi, J.C. Dharshan, R. Raghavendra, S.B. Telkar, *Med. Chem. Res*., **2013**, 22, 5814-5822.
[30] B. Sreekanth, G. Krishnamurthy, H.S. BhojyaNaik, T.K. Vishnuvardhan, *Nucleoside Nucleotides Nucleic Acids*., **2012**, 31, 1.
[31] A. Hall, D. Parsonage, L.B. Poole, P.A. Karplus, *J. Mol. Biol*., **2010**, 10, 194.
[32] W.A. Bayoumi, M.A. Elsayed, H.N. Baraka, L. Abou-zeid, *Arch. Pharm. Chem. Life. Sci*., **2012**, 345, 902.
[33] J.W. Visser, *J. Appl. Crystallogr*., **1969**, 2, 89-95.
[34] P.M. de Woulff, *J. Appl. Crystallogr*., **1968**, 1, 108-113.
[35] C.J. Dhanaraj, J. Johnson, *Spectrochim. Acta. A.*, **2014**, 118, 624-631.